TRW

The Potential for Ozone Depletion in Solid Rocket Motor Plumes by Heterogeneous Chemistry

Prepared for:

Prepared by:

M.S. Hanning-Lee and P.M. Felker

Department of Chemistry
University of California, Los Angeles, CA

and

J.A. Syage

Mechanics and Materials Technology Center
The Aerospace Corporation, Los Angeles, CA

Submitted by:

December 1995
(Revised: August 1996)

Report Documentation Page

Report Date	Report Type	Dates Covered (from... to)
00081996	N/A	-

Title and Subtitle	Contract Number
The Potential for Ozone Depletion in Solid Rocket Motor Plumes by Heterogeneous Chemistry	
	Grant Number
	Program Element Number

Author(s)	Project Number
Hanning-Lee, M.S., Felker, P.M., Syage, J.A.	
	Task Number
	Work Unit Number

Performing Organization Name(s) and Address(es)	Performing Organization Report Number
Department of Chemistry, University of California, Los Angeles, CA ; Mechanics and Materials Technology Center, The Aerospace Corporation, Los Angeles, CA	

Sponsoring/Monitoring Agency Name(s) and Address(es)	Sponsor/Monitor's Acronym(s)
Environmental Management Division, USAF Space and Missile Systems Center, El Segundo, CA	
	Sponsor/Monitor's Report Number(s)

Distribution/Availability Statement
Approved for public release, distribution unlimited

Supplementary Notes

Abstract

Subject Terms

Report Classification	Classification of this page
unclassified	unclassified

Classification of Abstract	Limitation of Abstract
unclassified	UU

Number of Pages
21

Summary

Rates of ozone decomposition on aluminum oxide (alumina) particles were measured in a flow tube reactor equipped with molecular beam sampling mass spectrometry and ultraviolet absorption spectroscopy, and in a static reaction cell equipped with ultraviolet absorption spectroscopy. Reaction probabilities η are reported for ozone on α-alumina, γ-alumina, and chromatographic alumina (hydroxylated alumina), respectively, over the temperature range -60 to 200°C. This work addresses the potential for stratospheric ozone depletion by launch vehicle solid rocket motor exhaust. Considering best estimates of plume particle size distributions and dispersion rates, we calculate ozone depletion profiles, for direct decomposition on alumina only. The calculated ozone holes are rather narrow. In the worst case, ozone levels are within 5×10^{-5} of ambient in the center of the plume. A simple analysis of the global impact of alumina particles on ozone decomposition indicates a potential steady-state daytime depletion of $<3\times10^{-9}$ at present launch rates.

The laboratory measurements presented here support atmospheric modeling efforts to understand rocket plume / stratosphere interactions. The laboratory and modeling work in turn is used to define design parameters for the HIgh Resolution Ozone ImaGing (HIROIG) spectrometer to be used to monitor ozone and chemical composition of solid rocket motor plumes.

1. Introduction

Solid rocket motors (SRM) are commonly used for heavy launch vehicles because of their high thrust, relatively uncomplicated and inexpensive construction, and because they use storable propellants (as opposed to cryogenic hydrogen/oxygen liquid thrusters). SRMs are the principal boosters on the four largest classes of US lifters, namely Space Shuttle, Titan IV, Delta, and Atlas. They are also to be used by the largest ESA launcher Ariane 5. The most widely used propellant formulation consists of ammonium perchlorate (NH_4ClO_4) oxidizer and aluminum (Al) fuel with organic binder.

Titan IV vehicles are launched by the USAF from Vandenberg AFB. A single Titan IV vehicle releases about 48 tons of chlorine and about 68 tons of alumina into the stratosphere (15-60 km). The quantity of material released by the Shuttle exhaust is about 30-40% greater. There is growing concern that this exhaust may contribute to ozone depletion in the stratosphere. There have been many attempts to model the impact of solid rocket motor plumes on stratospheric ozone. Prather and collaborators investigated the long term effects using global atmospheric chemistry and dispersion models from which they concluded that at current launch rates, solid rocket motor exhaust does not impose a significant global impact on stratospheric chemistry [*Prather et al.,* 1990a]. An attempt was also made to examine the transient chemical behavior and local impact. Subsequent discussions revealed a widely varying viewpoints [*Aftergood,* 1991; *McPeters et al.,* 1991].

Recently, a new understanding of plume chemistry has emerged that suggests the potential for short term ozone depletion along the path of SRM plumes. The principal reason is that much of the chlorine effluent is in the form of Cl_2 due to plume afterburning chemistry involving HCl and OH [*Hoshizaki,* 1975; *Karol,* 1992; *Zittel,* 1994; *Denison et al.* 1994]. Chemical kinetics modeling then predict extensive ozone depletion in the plume that persists for hours [*Denison et al.* 1994, *Karol,* 1991; *Ross,* 1995, *Brady and Martin,* 1995].

Measurements of plume composition are limited and inconclusive. A Titan III flythrough observed a 40% reduction in the ambient ozone level [*Pergament,* 1977], although this single

measurement has not be repeated. McPeters, et al. [1991] presented total ozone mapping images (TOMS) as evidence that ozone depletion is insignificant in the wake of a SRM plume. However, arguments have been presented indicating that TOMS is unable to measure such an effect due to limited spatial resolution, the complicating effects of plume species that overlap with the ozone absorption spectrum [*Syage*, 1995, *Syage and Ross*, 1996], and uncertainty concerning plume displacement due to stratopheric winds.

SRM motor plumes exhaust large quantities of aluminum oxide particles [*Brady et al.* 1994], so it is natural to consider whether heterogeneous chemistry, similar to that which occurs on polar stratospheric cloud (PSC) particles [*Solomon,* 1988, *Abbatt and Molina*, 1992; *Hanson and Ravishankara*, 1991, *Leu, Moore, and Keyser*, 1991], may also occur in rocket plumes. However, the plume environment differs from the Antarctic in several important ways: (1) alumina particles will probably have very different surface properties than PSCs, though adsorbed water may give rise to similar surface chemistry, (2) the stratospheric temperatures at mid latitudes are in the range of about 220-230K compared to 190-200K for the Antarctic winter, (3) the concentration of chlorine species is many orders of magnitude higher in the early plume than in the Antarctic, (4) potential for direct decomposition of ozone on alumina particles [Hanning-Lee, et al. 1996; Keyser, 1976], and (5) in the plume, photolysis on surfaces can compete with heterogeneous thermal chemistry, in contrast to the Antarctic where heterogeneous chemistry takes place mostly during the dark polar winter. The potential for heterogeneous photochemistry on alumina particles is the subject of this paper.

The laboratory measurements presented here support atmospheric modeling efforts to understand rocket plume / stratosphere interactions. The laboratory and modeling work in turn is used to define design parameters for the HIgh Resolution Ozone ImaGing (HIROIG) spectrometer to be used to monitor ozone and chemical composition of solid rocket motor plumes[*McKenzie, et al.,* 1993]. The work reported here was performed in a joint arrangement between UCLA and Aerospace and involved the efforts of Dr. Mark Hanning-Lee, a UCLA postdoc with Prof. Peter M. Felker, working at Aerospace under the supervision of Dr. Jack A. Syage. Aerospace facilities and resources, under AFSMC/CEV funding, contributed to this work.

2. Ozone decomposition on alumina

In this section, we present measurements of rates of ozone decomposition on aluminum oxide (alumina) particles. The purpose of this work is to examine the extent to which ozone would be depleted due to solid rocket motor (SRM) alumina particle exhaust. This question necessarily involves the coupling with other ozone depleting chemistry, such as homogeneous and heterogeneous chlorine chemistry. However, it is also important to isolate the reactivity of ozone with alumina because of the importance of evaluating (i) long-term global ozone impacts, and (ii) future propellant formulations that dispense with chlorine, but which retain aluminum.

A single Titan IV vehicle releases about 48 tons of chlorine and about 68 tons of alumina into the stratosphere (15-60 km) [*Brady et al* 1994]. The quantity of material released by the Shuttle exhaust is about 30-40% greater. At present, the magnitude of ozone depletion in SRM plumes is not accurately known. Chemical modeling calculations indicate the potential for significant local ozone depletion [*Karol*, 1992; *Zittel*, 1994; *Denison et al.* 1994; *Ross*, 1995; *Brady and Martin*, 1995], however, many key reaction rates are as yet still unmeasured. The importance of heterogeneous chemistry on alumina particles is also a very open question.

Properties of alumina particles in the plume, e.g., size distributions, densities, surface structure, and composition are poorly understood, yet these factors will strongly influence chemical reactivity. Some of these properties have been studied for tropospheric alumina exhaust [*Radke, Hobbs, and Hegg*, 1982; *Kim, Laredo, and Netzer*, 1993; *Strand*, 1981, *Cofer et al*, 1987, 1991]. SRM plumes may consist of high densities of transient ice crystals solidified from the exhaust as neat particles or coated on alumina. The heterogeneous chemistry of these plume particles is just beginning to be examined [*Lohn et al.* 1994; *Syage and Ross*, 1996]. Since surface chemistry may be catalytic in nature, these particles may potentially have an impact on stratospheric plume chemistry similar to that observed in polar stratospheric clouds (PSCs) in the Antarctic.

If one assumes pseudo-first-order kinetics with respect to ozone, then reaction efficiency η can be related to rate constant k by the expression

$$\frac{d\ln[O_3]}{dt} = -k[Al_2O_3] = -\frac{v\eta\Sigma}{4}[Al_2O_3] \qquad (2.1)$$

where v is the mean molecular speed of O_3, Σ is the surface area per unit mass of alumina and $[Al_2O_3]$ is mass per unit gas-phase volume. The most comprehensive measurements to date appear to be those by Keyser [1977] in a JPL report. He reported reaction efficiencies measured by static and flow methods for different alumina surfaces, after adsorption of H_2O and HCl, and over a temperature range of -40 to 40°C. Keyser [1991, 1993] considered the details of diffusion and adsorption and how well ozone accesses the total surface area of porous alumina. The surface reactivities he reported of $\eta \sim 10^{-9}$ (at room temperature) are several orders of magnitude smaller than those reported by other groups. Early work by flow methods report values of $\eta \sim 10^{-5}$ [*Schwab and Hartmann*, 1956; *Ellis and Tometz*, 1972; *Atiaksheva and Emelianova*, 1973]. More recently Klimovskii et al. [1983] reported an ozone reactivity of $\eta \sim 10^{-4}$ at room temperature. The issue of particle porosity and effective surface area is a key issue in the present work in comparing reactivity of laboratory particles to plume alumina exhaust. Of the previous measurements of O_3 reactivity on alumina particles, only the results of Keyser and of Alebic-Juretic *et al.* [1992] allow determinations of reactivity as a function of surface area defined by the BET isotherm.

2.1. Experimental

The measurements presented here were conducted using a flow-tube reactor equipped with a molecular beam sampling mass spectrometer and an ultraviolet/vacuum ultraviolet absorption spectrometer as illustrated in Fig. 2.1. Details of the apparatus will be presented elsewhere [*Hanning-Lee et al.*, 1996]. The flow tube consists of a jacketed pyrex tube through which temperature-controlled solvent is passed to achieve temperatures from -70 to 25°C. The flow tube is contained in an oven. In this work temperatures up to 200°C were achieved by draining the cooling solvent and heating the tube in the oven. An alumina sample was inserted
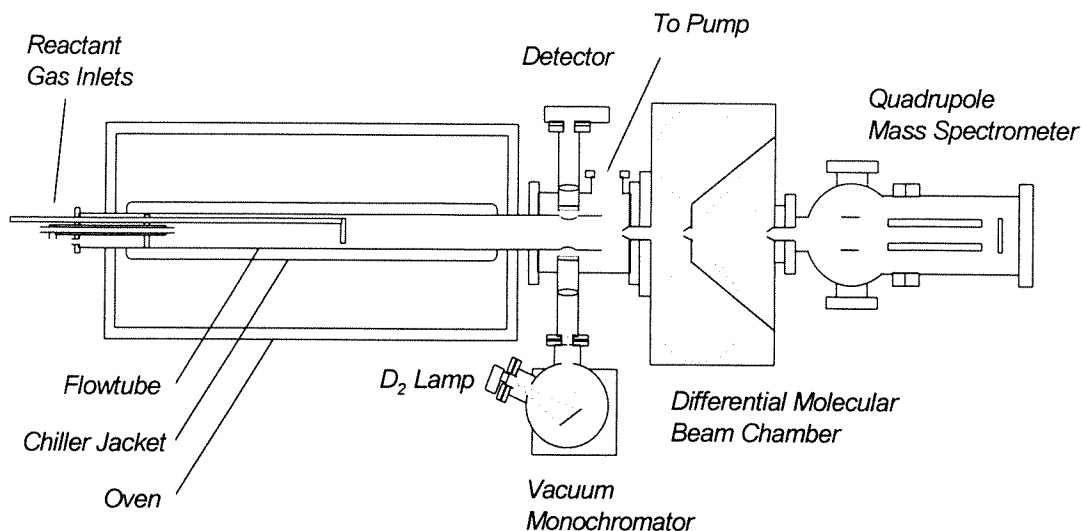
Figure 2.1. Diagram of the flow tube reactor, molecular beam sampling, mass spectrometer. The apparatus is also equipped with an absorption spectrometer. Aluminum oxide sample is inserted in a 36 in long by 0.75 in wide trough that sits on the bottom of

along the length of the flow tube, in as thin a layer as possible, in a glass, stainless steel, or aluminum sample trough 0.75 in wide and 36 in long. An O_2/O_3 mixture was introduced into a carrier flow through an injector that can be moved to different positions so as to vary the time for which O_3 is in contact with the alumina sample. The carrier flow was He with 0.3% Ar added as an internal standard for the mass spectrometer. Some samples were saturated with HCl (as determined by the HCl mass signal reach stead state).

Rate constants were measured over a temperature range of $-60°C$ to $200°C$ for three types of alumina: (1) α-alumina, 3 mm diam particles (Aldrich), (2) γ-alumina, 3 mm diam particles (Aldrich), and (3) chromatographic (partially hydroxylated) alumina, 0.25 mm diam particles (Alfa). Control measurements were also made in the absence of sample, which were used to correct the reported rate constants. All measurements used simultaneous mass spectrometric and UV absorption monitoring of ozone concentration. UV absorption was typically measured at a wavelength chosen to achieve an optical density of about unity, for optimum sensitivity to small changes in ozone concentration. The mass spectrometer and UV absorption methods gave consistent results in all cases; however, the latter tended to give better reproducibility
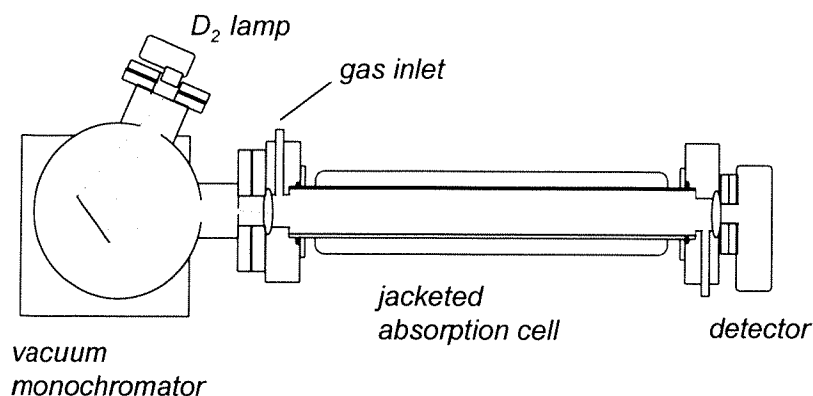
Figure 2.2. Schematic of the static cell kinetic absorption spectrometer. The cell is jacketed to allow measurements over the temperature range of 220 to 350 K.

and sensitivity. Homogeneous O_3 loss is at least a factor of 10 smaller than the rates measured here.

Surface area is defined as the geometric, or outside, surface area and not the total effective surface area due to a porous structure. The geometric surface area was computed from the measured weight and known density and particle size distribution of the sample. The issue of the *effective* surface area is a difficult one to deal with. Using the chemical supplier's porosity data, the ratio of internal surface area to the geometric outside surface area is $\geq 10^4$ for chromatographic alumina. When reporting values of η, it is important to be consistent in the definition of surface area. Because we do not know the effective surface area for ozone decomposition, nor do we know the porosity of plume particles, we choose to define reactivity in terms of the simple concept of geometric or external surface area. The values of η presented here are directly applicable to calculating ozone decomposition in SRM plumes as long as we are consistent by dealing with the geometric surface area of the plume particles. This approach is fully valid for assessing the plume issue if the porosity of the laboratory and plume particles are equivalent.

A new apparatus was constructed that is better suited than a flow tube reactor for measuring slow reactions. The apparatus employs real-time absorption monitoring in a static reaction chamber as illustrated in Fig. 2.2. Measurements are made by injecting a reaction mixture to the chamber containing some alumina sample and measuring the rate of change of gas composition by absorption. The minimum reaction time is limited by the time it takes to add the
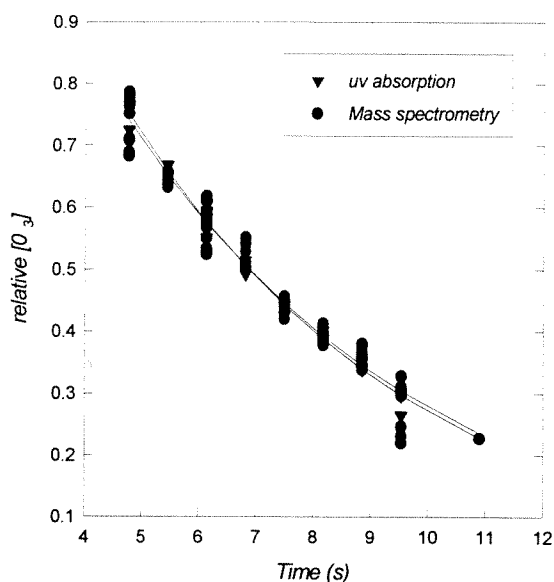
0.9

0.8 — ▼ uv absorption
0.7 — ● Mass spectrometry

relative [O₃]

Figure 2.3. Kinetics trace recorded for γ-alumina at 200°C.

reaction mixture (about 1 sec). The effective temperature range is -50°C to 100°C using temperature controlled liquid flows through the cell jacket, and up to 200°C using heating tape. The advantages of the static reaction chamber in Fig. 2.2 are (i) the absorption of reactant or product is followed in real-time and (ii) sample can be rapidly and efficiently changed. The disadvantage is that it is not appropriate to measuring fast reactions. The flow tube reactor and the static reaction chamber are very complementary instruments and operate well over a wide range of overlapping conditions allowing comparisons of measured reaction rates by two independent methods.

2.2. Results and Analysis

An example of a kinetics decay trace recorded using mass spectrometric and absorption measurements is given in Fig. 2.3. A compilation of results of kinetics measurements of ozone decomposition on various types of alumina and surface coatings are plotted in Fig. 2.4. The order of ozone reactivity is γ-alumina > chromatographic alumina > α-alumina. The reaction probabilities in Fig. 2.4a for ozone on dry γ-alumina are 3×10^{-4}, 8×10^{-5}, and 4×10^{-4} (1σ uncertainty of ±40%) at −60, 20, and 200°C, respectively. The γ-alumina is about an order of magnitude more reactive to ozone than is α-alumina (the latter results are not shown). When experiments on dry γ-alumina were repeated two months later, the rates decreased by an average of 40-50% (Fig. 2.4), which is in the range of the stated error limits. These latter measurements were conducted in concert with measurements on γ-alumina saturated with HCl. The results in Fig. 2.4b show that HCl reduces the rate of ozone decomposition, possibly by binding to alumina surface sites that are reactive to ozone. HCl increases the Bronsted acidity of
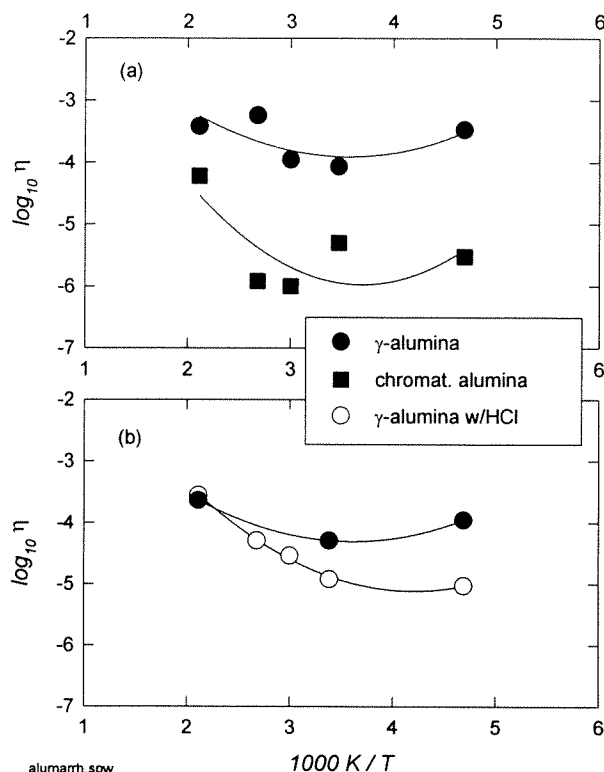
Figure 2.4. Temperature dependence of ozone reactivity on (a) 3 mm diam γ-alumina particles and on powdered chromatographic alumina, and (b) 3 mm diam γ-alumina particles with and without adsorbed HCl. Quadratic fit is for visualization only. 1σ error limit is about ±40%, which is on the order of scatter from the quadratic fit. [*Hanning-Lee et al.*, 1996a]

alumina surface [*Tanaka and Ogasawara*, 1969]. It is known that ozone decomposition is favored by high pH in aqueous solution, so HCl might be expected to deactivate alumina for ozone decomposition. Preliminary experiments for H_2O adsorption show a similar deactivation of ozone decomposition. In an early SRM plume, alumina is expected to become coated with HCl and H_2O. However, as the plume disperses, these adsorbates will evaporate.

There is a noticeably U-shaped dependence of log η vs $1/T$ in Fig. 2.4. The high temperature dependence can be described by an activated Arrhenius dependence, whereas the increase in rate at low temperatures is attributed to longer residence times of adsorbed O_3 on the surface. In a sense, the alumina particles act as a sorption pump at stratospheric temperatures, thereby increasing the time during which O_3 can react with the surface. The lack of an upturn in ozone decomposition rate at −60°C for HCl-coated alumina (Fig. 2.4b) reflects the increased adsorption efficiency of HCl at low temperatures.

The results measured here differ in some respects from those reported by Keyser [1977]. Our ozone decomposition rates are about an order of magnitude greater than in the earlier study after normalizing to the same definition of surface area. Furthermore, the upturn in rate at lower temperature and the deactivation of rate for HCl saturated particles is not observed in the Keyser study. One major difference between the two studies is that we used a loose col-
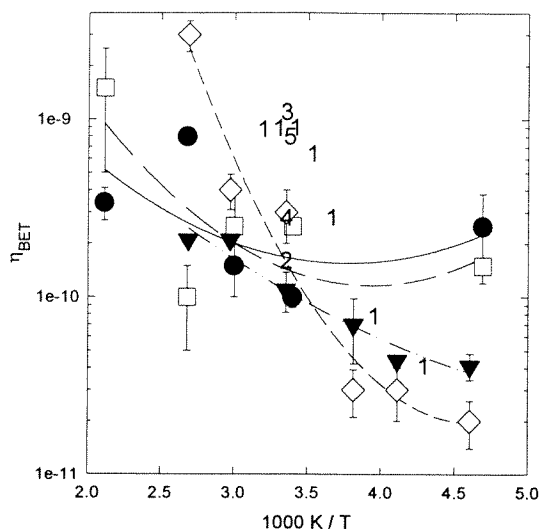
Figure 2.5. Temperature dependence of ozone reactivity on alumina particles. Quadratic fit is for visualization only. Error bars reflect statistical 1σ error. Values for α chips are lower limit. Key: 1-4 Keyser samples A-D, 5 Alebic-Juretic *et al.* [1992]. ●: flow tube coarse γ. ▢: flow tube chromatographic γ. ▼: static cell coarse γ. ◇: α chips.

lection of particles of uniformly large size to avoid packing, whereas Keyser employed a packed flow column. However, the latter work has considered the effects of diffusion in detail. Although he corrects for diffusion effects. The possibility of an ozone diffusion limitation between particles due to close packing of particles in our flow tube was investigated. For the chromatographic alumina sample (0.25-mm diam particles), we observed a factor of two increase in rate for a 25-50% reduction in pressure indicating a diffusion limitation. The rates for chromatographic alumina should, therefore, be considered a lower limit. A similar experiment for the 3-mm diam γ-alumina particles gave no evidence of a diffusion limit.

After this project ended, we obtained additional results relating O_3 decomposition as a function of BET surface area. These results are presented in Hanning-Lee et al. [1996] and summarized in Fig. 2.5.

2.3. Impact of Surface Reactivity on Ozone Depletion in the Stratosphere

Local Impact

Here we consider the local impact of alumina particles on stratospheric ozone depletion based on our measured values of η. We define a time constant for first-order ozone decomposition from Eq. (2.1)

10

$$\tau \ = \ \frac{1}{k[Al_2O_3]} \ = \ \frac{4}{\nu\eta\,\Sigma\,[Al_2O_3]} \tag{2.2}$$

Our measurements validate the assumption of first-order kinetics. Eq. (2.2) is adequate for modeling a constant environment where $[Al_2O_3]$ is fixed in time (e.g., in a flow tube reactor). In the plume, $[Al_2O_3]$ decreases with time because of expansion and dispersion. We describe the time dependence by the function

$$c(t) \ = \ \frac{D}{A(t)} \tag{2.3}$$

where $c(t) = [Al_2O_3]$ at time t, D is the deposition rate (mass/distance) of alumina into the stratosphere and $A(t)$ is the cross sectional area of the plume calculated for some assumed dispersion model. For a Titan IV/SRMU, D has a value of 3.9 and 2.6 tons/km at 20 and 30 km altitude, respectively. Eq. (2.3) assumes that the density of alumina is uniform within the cross sectional area of the plume. A more realistic distribution (e.g., Gaussian) requires additional computation. Integrating Eq. (2.1) leads to the expression

$$\ln\frac{[O_3]_\infty}{[O_3]_0} \ = \ -\frac{\nu\eta\Sigma D}{4}\int\limits_0^\infty A(t)^{-1}\,dt \tag{2.4}$$

where $[O_3]_0$ is the ambient ozone concentration and $[O_3]_\infty$ is the remaining ozone after the plume has completely dispersed. This simple model does not assume any other dynamics, such as the recovery of ozone in the plume track by mixing with ambient atmosphere. Eq. (2.4) basically describes the competition between ozone depletion and plume dispersion. If dispersion is much slower than reaction, then $A(t)$ is essentially constant and the ozone will decay by first-order kinetics to zero. If dispersion is much faster than reaction, then ozone concentration will reach a non-zero value.

Beiting [1995] has compared dispersion models used by different investigators and finds that they can be approximated by a linear function $d=2at$ where d is the plume diameter, and a is the radial expansion rate. The plume cross sectional area can then be represented as

$$A(t) = \pi(r_0 + at)^2 \qquad (2.5)$$

where r_0 is the initial plume radius after expanding out of the nozzles. Evaluating Eq. (2.4) leads to the expression

$$\frac{[O_3]_\infty}{[O_3]_0} = \exp\left\{-\frac{\nu\eta\Sigma D}{8\pi a r_0}\right\} \qquad (2.6)$$

As a result of the assumption of uniform concentration of alumina within the plume cross sectional area, Eq. (2.6) essentially describes the extent of ozone depletion at position r_0 in the initial plume exhaust. The spatial distribution of ozone depletion away from the plume centerline may be evaluated by varying the value of r_0. This is equivalent to allowing the plume to expand to a specific radius r and then starting the kinetics integration, thereby calculating the total ozone reacted at that position as the plume expands to infinity.

There is still considerable uncertainty regarding particle size distributions and dispersion rates in stratospheric plumes. Based a recent analysis of SRM alumina particle size distribution and uncertainty [*Beiting*, 1995], one obtains a range of BET surface areas of 5×10^4 to 10^6 cm^2/g depending on whether one assumes pure α- or γ-alumina samples.. With regard to dispersion rates, Beiting [1995] has noted that there is a large variation in dispersion rates used by different investigators to model plumes. Brady and Martin calculated plume kinetics over a large range of expansion rates and find that the severity of an ozone hole increases with decreasing plume expansion rate, in agreement with this simple model. They then provided detailed calculations for an expansion rate of about $a = 1.4$ km/hr based on a plume dispersion model by Watson *et al.* [1978]. Ross [1995] and Denison *et al.*[1994] chose values of a of 1.5 km/hr (at 20 km) and 12 km/hr, respectively. Beiting [1995] noted that a visual analysis of the expansion rate of a Titan IV plume at 20-30 km yields about 17 km/hr over the first 10 min, after which the plume was not visible to the eye.

For our calculations, we assume a mid-latitude stratospheric temperature of $-60°$C and use our measurement for γ-alumina activity of $\eta_{BET} = 3\times10^{-10}$. Calculations of ozone depletion profiles are plotted in Fig. 2.6 for a wide range of a and Σ values. Depending on the set of as-
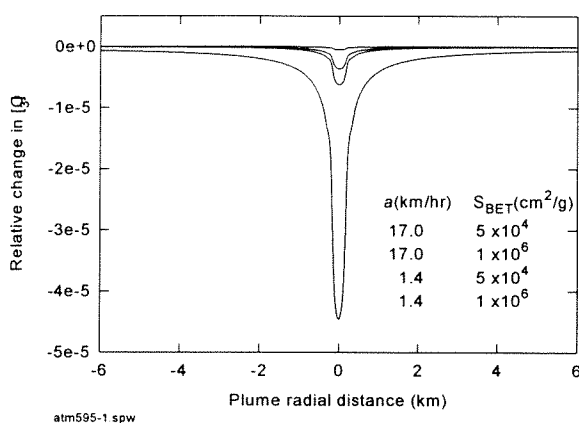
Figure 2.6. Radial distribution for ozone depletion relative to ambient level for various models of plume expansion rate *a* and specific surface area of particles Σ. The table of input parameters appear in the same order as the calculated curves.

sumed values for *a* and Σ, the local ozone depletion problem ranges from minuscule to moderately severe. The peak ozone depletions in Fig. 2.6 range from about 10^{-4} to 10^{-6} of ambient. The ozone holes are relatively narrow, about 400 m. Sophisticated chemical kinetics models predict greater ozone losses due to homogeneous chlorine, NO_x, and HO_x chemistry [*Karol*, 1992; *Zittel*, 1994; *Denison et al.* 1994; *Ross*, 1995; *Brady and Martin*, 1995]. The effect of alumina reactivity under these more complicated chemical conditions must be tested using these kinetics models.

The uncertainty in our combined understanding of reaction rates, plume particle properties (i.e., size, phase, surface properties), plume dispersion rates, and other chemical interactions, is still too large to rule out the possibility of a significant problem. On the other hand, there are several possible plume properties that would lessen the severity of the alumina decomposition problem, such as: (i) increased proportion of α-alumina, (ii) increased proportion of large particles which would reduce Σ, (iii) H_2O or HCl-coated alumina, (iv) plume dispersion rates greater than previously assumed [*Beiting*, 1995], and (v) ozone recovery due to mixing with ambient air.

Global Impact

We now consider the global impact of alumina on ozone decomposition. A proper analysis should consider deorbiting debris and alumina injection by launch vehicles; we consider just the latter. We also exclude in this simple analysis the effect of alumina particles on reservoir

13

species, and the effect of sulfate adsorption on alumina. The steady-state concentration of alumina (mass/volume) is given by

$$[Al_2O_3]_{ss} = \frac{\kappa \tau_s}{V} \qquad (2.7)$$

where κ is the alumina deposition rate (mass/yr) into the stratosphere due to SRM launch vehicles, τ_s is the particle settling time (yr), and V is the global volume of the stratosphere. The total deposition rate of alumina into a 15-60 km band for all worldwide launches is reported to be $\kappa = 1.5 \times 10^6$ kg/yr [1993-97 rate from *Brady et al.*, 1994]. The removal time is more difficult to estimate because it depends on particle size and altitude. Removal rates are a function of eddy diffusion (dominant for <0.1 μm particle size) and gravitational settling (dominant for >1 μm particle size). The rate of gravitational settling under viscous drag is given by Stokes' formula

$$\tau_s^{-1} = \frac{2}{9} \frac{r^2 \rho g}{\eta} \left(1 + A\frac{\lambda}{r}\right) \qquad (2.8)$$

where r and ρ are the particle radius and density, respectively, g is the gravitational acceleration, η is viscosity (not to be confused with reaction efficiency η defined earlier), λ is the mean free path of gas molecules, and A is a factor on the order of unity [*Fuchs*, 1964]. Using the viscosity of air at -60°C of 130 μP, one obtains settling rates of 0.012 cm/s and 1.2×10^{-4} cm/s for 1 μm and 0.1 μm diameter alumina particles, respectively. These particle sizes are typical of the plume [*Beiting*, 1995]. Over small spatial scales, the settling rate of aerosols at 1 atm pressure is calculated to go through a minimum value of 10^{-3} cm/s for particle diameters 0.1-1.0 μm [*EPA*, 1975], the lower size limit being determined by Brownian motion. Using this settling rate for 0.1 μm particles and the above calculated rate for 1 μm particles leads to settling rates in the viscous regime in the stratosphere of about 30 yr and 3 yr, respectively. It is unlikely, however, that Brownian diffusion is relevant over kilometer distances. Instead, factors that would reduce these times are eddy diffusion in the stratosphere and molecular flow conditions in the upper stratosphere.

Eddy diffusion was evaluated by Watson *et al.* [1978] for plume dispersion and fallout. Using a compilation of the best models available, they determined stratospheric residence times ranging from 2.5 to 5 years for particles originating at altitudes of 20 to 30 km, respectively. Interestingly, the residence time does not increase substantially above 30 km (it is a constant 5.5 years from 60-100 km) indicating that material falls or diffuses rapidly from the upper stratosphere to the lower stratosphere where it then persists. The same trend is also predicted for large particle settling by Eq. (2.8). The mean free path is related to molecular number density n, by the relation $\lambda = 1/\pi d^2 n$ (d is molecular diameter). Eq. (2.8) states that τ_s^{-1} is constant at high pressure (i.e., high number density), but increases linearly with inverse pressure at low pressure. The minimum in the dependence corresponds to $\lambda \cong r$. This condition occurs in the troposphere for 0.1 μm particles and the lower stratosphere for 1 μm particles.

For our analysis, we will use a typical residence time of $\tau_s = 3$ yr. The stratospheric volume is given by $V = 4\pi r^2 \Delta r$ where r is the Earth's radius and Δr is the effective thickness of the alumina band in the stratosphere. As discussed above, we assume that the alumina settles into the lowest 15 km of the stratosphere (15-30 km), which is where ozone density is greatest. This gives a value of $V = 7.7 \times 10^9$ km^3. The steady-state concentration of alumina in the global stratosphere is then $[Al_2O_3]_{ss} = 5.8 \times 10^{-16}$ g/cm^3. Using Eq. (2.2) and values of $\eta_{BET} = 2 \times 10^{-10}$ and $\Sigma_{BET} = 10^6$ cm^2/g gives an ozone decay rate of 8.9×10^{-16} s^{-1}, corresponding to a lifetime τ of 36 Myr. To calculate how this rate of depletion affects the ozone balance, we begin with a simple expression for the steady state concentration of ozone by the Chapman cycle given by [*Wayne*, 1991]

$$[O_3] + [O] = \left(\frac{2 J_{O2} [O_2]}{k_{O2}} \right)^{1/2} \tag{2.9}$$

Below 34 km, $[O_3]$ exceeds $[O]$ by more than an order of magnitude. The change in $[O_3]$ due to the addition of an alumina decomposition term that competes with the loss term in the oxygen-only cycle is given by

15

$$\frac{\Delta[O_3]}{[O_3]} = 1 - \left(\frac{k_{O2}[O]}{k_{O2}[O]+\tau^{-1}}\right)^{1/2} \qquad (2.10)$$

The product $k_{O2}[O]$ ranges from 1.4×10^{-7} to 3×10^{-6} s^{-1} for 20 to 30 km altitude, respectively. This gives a value of $\Delta[O_3]/[O_3]$ ranging from 3×10^{-9} to $<10^{-9}$.

2.4. Summary and Conclusion

Rates of ozone decomposition on aluminum oxide particles were measured in a flow tube reactor equipped with molecular beam sampling mass spectrometry and ultraviolet absorption spectroscopy. The order of reactivity is γ-alumina > chromatographic alumina > α-alumina. The reaction probabilities for ozone on dry γ-alumina are 3×10^{-4}, 8×10^{-5}, and 4×10^{-4} (±40%) at −60, 20, and 200°C, respectively. Adsorption of water reduces the surface activity by about an order of magnitude. Saturation with HCl reduces surface activity by an order of magnitude at −60°C and has little effect above 60°C (presumably due to the lower steady-state HCl surface coverage).

This work addresses the potential for ozone depleting chemistry in the stratosphere from launch vehicle solid rocket motor exhaust. There are still large uncertainties in our knowledge of plume particle size distributions and dispersion rates. Using a range of estimates for these plume properties, we calculate a centerline ozone depletion ranging from 1×10^{-6} to 5×10^{-5} due to direct decomposition on alumina only. The ozone holes are relatively narrow. In the worst case, ozone levels are depleted by less than 10% of ambient at 4 km from centerline. A simple analysis of the global impact of alumina particles on ozone decomposition indicates a potential steady-state depletion of 10^{-9} at present launch rates. A better analysis of this potential problem requires an understanding of the surface properties of exhaust alumina at long times, the true rate of plume dispersion, the effect of alumina particles on reservoir species, and the effect of sulfate adsorption on alumina.

3. Acknowledgements

Note added for revision

During the period of time since the original submission of the Final Report in December 1995 marking the end of the project, and this revised Final Report, further measurements and stratospheric assessments were made. Some of these results were incorporated in this Final Report for the sake of currency. However, one should refer to the paper Hanning-Lee et al. [1996] for the latest results and assessments of the plume/stratosphere impact.

4. References

Abbatt, J. P. D., and M. J. Molina, "Heterogeneous interactions of $ClONO_2$ and HCl on nitric acid trihydrate at 202 K," *J. Phys. Chem.* **96**, 7674 (1992).

Aftergood, S., "Comment on 'The space shuttle's impact on the stratosphere' by M. J. Prather et al.," *J. Geophys. Res.* **96**, 17,377 (1991).

Alebic-Juretic, A., T. Cvitas, and L. Klasinc, "Ozone destruction on powders", *Ber. Bunsenges. Phys. Chem.* **96**, 493 (1992).

Atiaksheva, L. F., and G. I. Emelianova, *Zh. Fizich. Khim.* **47**, 2113 (1973).

Bailey, R. R., and J. P. Wightman, "Interaction of gaseous hydrogen chloride and water with oxide surfaces," *J. Colloid Interface Sci.* **70**, 112 (1979).

Beiting, E. J., "Characteristics of alumina particles from solid rocket motor exhaust in the stratosphere," The Aerospace Corporation, TR-95(5231-16)-8 (xxxx, 1995).

Brady, B. B., and L. R. Martin, "Modeling solid rocket booster exhaust plumes in the stratosphere with SURFACE CHEMKIN," The Aerospace Corporation, TR-95(5231)-9 (xxxx, 1995).

Brady, B. B., E. W. Fournier, L. R. Martin, and R. B. Cohen, "Stratospheric ozone reactive chemicals generated by space launches worldwide," The Aerospace Corporation, TR-94(4231)-6 (SMC-TR-94-42) (Nov 1, 1994).

Cofer III, W. R., G. G. Lala, and J. P. Wightman, "Analysis of mid-tropospheric space shuttle exhausted aluminum oxide particles," *Atmos. Environ.* **21**, 1187 (1987).

Cofer III, W. R., G. C. Purgold, E. L. Winstead, and R. A. Edahl, "Space shuttle exhausted aluminum oxide," *J. Geophys. Res.* **96**, 17,371 (1991).

Denison, M. R., J. J. Lamb, W. D. Bjorndahl, E. Y. Wong, and P. D. Lohn, "Solid rocket exhaust in the stratosphere: Plume diffusion and chemical reaction," *J. Spacecraft & Rocket*, **31**, 436 (1994).

Dillard, J. G., R. D. Seals, and J. P. Wrightman, "Electron spectroscopy for chemical analysis (ESCA) study of aluminum-containing atmospheric particles," *Atm. Environ.* **14**, 129 (1980).

Dunn, R. C., J. D. Simon, "Excited-state photoreactions of chlorine dioxide in water," *J. Am. Chem. Soc.* **114**, 4856, (1992).

Ellis, W. D., and P. V. Tometz, "Room temperature catalytic decomposition of ozone," *Atmos. Environ.* **6**, 707 (1972).

EPA, "Position paper on regulation of atmospheric sulfates," Environmental Protection Agency, Report EPA-450/2-75-007 (Sept 1975).

Fuchs, N. A., "The mechanics of aerosols," (Dover Publications, New York, 1964), pp. 21ff.

Hanning-Lee, M. A., B. B. Brady, L. R. Martin, and J. A. Syage, "Ozone decomposition on alumina: Implications for solid rocket motor exhaust," *Geophys. Res. Lett.*, **23**. 1961 (1996).

Hanning-Lee, M. A., B. B. Brady, and J. A. Syage, "Kinetics of ozone decomposition on aluminum oxide particles," *J. Phys. Chem.*, to be submitted (1996).

Hanson, D. R., and A. R. Ravishankara, "The reaction probability of $ClONO_2$ and N_2O_5 on polar stratospheric cloud materials," *J. Geophys. Res.* **96**, 5081 (1991).

Hoshizaki, H. (chairman), "Aircraft wake microscale phenomena," *in The Stratosphere Perturbed by Propulsion Effluents, CIAP Monogr.* 3, chap. 2., pp. 60-73, Climatic Impact Assessment Program, U.S. Dept. of Transportation, Washington D. C., Sept. 1975.

Karol, I. L., Y. E. Ozolin, and E. V. Rozanov, "Effect of space rocket launches on ozone," *Ann. Geophysicae* **10**, 810 (1992).

Keyser, L. F., "Heterogeneous reaction of ozone with aluminum oxide," *JPL Technical Memorandum* 33-782 (August 15, 1976).

Keyser, L. F., S. B. Moore, and M.-T. Leu, "Surface reaction and pore diffusion in flow-tube reactors," *J. Phys. Chem.* **95**, 5496 (1991).

Keyser, L. F., and M.-T. Leu, "Surface areas and porosities of ices used to simulate stratospheric clouds," *J. Colloid Interface Sci.* **155**, 137 (1993).

Klimovskii, A. O., A. V. Bavin, V. S. Tkalich, and A. A. Lisachenko, "Interaction of ozone with γ-Al_2O_3 surface," *React. Kinet. Catal. Lett.* **23**, 95 (1983).

Kim, H.-O., D. Laredo, and D. W. Netzer, "Measurement of submicrometer Al_2O_3 particles in plumes," *Appl. Opt.* **32**, 6834 (1993).

Leu, M.-T., S. B. Moore, and L. T. Keyser, "Heterogeneous reactions of chlorine nitrate and hydrogen chloride on type I polar stratospheric clouds," *J. Phys. Chem.* **95**, 7763 (1991).

Levine, I. N., "Physical Chemistry," McGraw-Hill, New York, 1978.

Lohn, P. D., E. Y. Wong, M. J. Molina, and M. R. Denison, "The impact of deorbiting space debris on stratospheric ozone," TRW Engineering Report, CDRL No. A005-2 (May 31 1994).

McKenzie, D. L., et al., "System requirements for the high-resolution ozone imager (HIROIG)," The Aerospace Corporation, TR-93(3231)-2 (Sept. 15, 1993).

McPeters, R., M. Prather, and S. Doiron, "Reply," *J. Geophys. Res.* **96**, 17,379 (1991).

Pergament, H. S., R. I. Gomberg, and I. G. Poppoff, "NO_x deposition in the stratosphere from the space shuttle rocket motors," Appendix G to *NASA Tech. Memo.* X-58198, G-3, Jan. 1977.

Prather, M. J., M. M. Garcia, A. R. Douglass, C. H. Jackman, M. K. W. Ko, and N. D. Sze, "The space shuttle's impact on the stratosphere," *J. Geophys. Res.* **95**, 18,583 (1990).

Radke, L. F., P. V. Hobbs, and D. A. Hegg, "Aerosols and trace gases in the effluents produced by the launch of large liquid- and solid-fueled rockets," *J. Appl. Meteor.* **21**, 1332 (1982).

Ross, M., "Local impact of large solid rocket motor exhaust on stratospheric ozone and surface ultraviolet flux," *J. Spacecraft & Rocket*, in press (1995).

Schwab, G. M., and G. Hartmann, *Z. Physik. Chem.* **6**, 56 (1956).

Solomon, S., "The mystery of the Antarctic ozone hole," *Rev. Geophys.* **26**, 131 (1988).

Strand, L. D., J. M. Bowyer, G. Varsi, E. G. Laue, and R. Gauldin, "Characteristics of particles in the exhaust plume of large-solid propellant rockets," *J. Spacecraft & Rocket* **18**, 297 (1981).

Syage, J. A., "Can the total ozone mapping spectrometer (TOMS) measure ozone depletion in rocket plumes," The Aerospace Corporation, TR-95(5231)-4 (SMC-TR-95-31) (1 June 1995).

Syage, J. A., M. A. Ross "An assessment of the total ozone mapping spectrometer for measuring ozone levels in a solid rocket motor plume", *Geophys. Res. Lett.*, in press (1996)

Taube, H., "Photochemical reactions in solution," *Trans. Faraday Soc.* **53**, 656 (1957).

Watson, R. T., P. E. Smokler, and W. B. DeMore, "An assessment of an F_2 or N_2O_4 atmospheric injection from an aborted space shuttle mission," JPL Publication 77-81 (April 15, 1978).

Zittel, P. F., "Computer model predictions of the local effects of large, solid-fuel rocket motors on stratospheric ozone," The Aerospace Corporation, TR-94(4231)-9 (SMC-TR-94-36) (Sept 10, 1994).